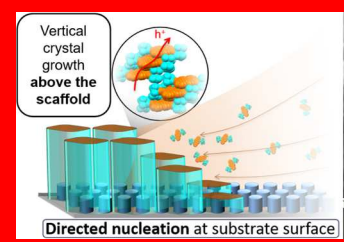


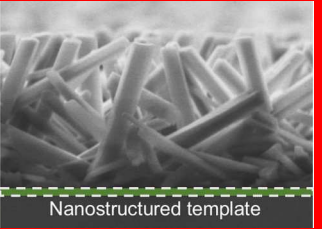
Directing Solution-Phase Nucleation To Form Organic Semiconductor Vertical Crystal Arrays

Kai Zong,[†] Yichen Ma,[‡] Kamran Shayan,[‡] Jack Ly,[§] Emily Renjilian,[†] Chunhua Hu,^{||} Stefan Strauf,[‡] Alejandro Briseño, and Stephanie S. Lee*, 10

Supporting Information

Control over the out-of-plane molecular orientation of solution-processed organic semiconductors is a long-standing challenge in the organic electronics community. Here, a generalizable strategy using nanoconfinement to direct the nucleation of small-molecule organic semiconductors during solution-phase deposition is presented. Using a facile dip-coating process, triisopropylsilylethynylderivatized acene molecules were deposited onto nanoporous anodized aluminum oxide (AAO) scaffolds with average pore





diameters ranging from 60 to 200 nm. Preferentially oriented nuclei were found to form within the cylindrical AAO nanopores such that the fast growth direction (i.e., the π -stack direction) aligned with the long axes of the pores. Crystal growth then propagated above the scaffold, resulting in the formation of vertical crystal arrays with the high surface energy π-planes exposed at the crystal tips. The diameters and heights of these crystals were tunable over ranges of 100-600 nm and 0.8-6.7 μ m, respectively, by varying the dip-coating speed and scaffold pore diameters. Photoluminescence (PL) experiments further revealed an 8-fold enhancement of the PL signal from vertical crystal arrays compared to horizontal crystals deposited on flat SiO₂ substrates due to waveguiding along the crystal length. Critically, this strategy is compatible with continuous deposition techniques that will enable the high-throughput, large-area manufacturing of flexible and inexpensive optoelectronic devices.

■ INTRODUCTION

Soluble small-molecule semiconductors, in which bulky insulating substituents are attached to insoluble electricallyactive cores, take advantage of the ease of solution processing afforded by semiconducting polymers while retaining the high degree of crystallinity exhibited by small-molecule systems compared to polymers. Such molecules have revolutionized the field of organic electronics, leading to solution-processed organic field-effect transistors (OFETs) with mobilities exceeding 1 cm²/V·s. Pioneered by the Anthony group in 2001, 1,2 one of the most successful design strategies to-date has been the incorporation of solubilizing rigid silyl groups to electrically and optically active acene cores. This strategy is exemplified in triisopropylsilylethynyl pentacene (TIPS-PEN), which has garnered thousands of articles over the past two decades as one of the most promising active materials for easily processed OFETs.3,4

In addition to altering molecular properties (e.g., solubility in organic solvents) and crystal properties (e.g., packing motifs and molecular spacings), the incorporation of bulky insulating groups to semiconducting molecules necessarily affects

molecule-substrate interactions during film deposition, and thus molecular orientation. Controlling the out-of-plane orientation of these molecules during solution deposition remains an outstanding, critical challenge in this field. For example, while thermally evaporated pentacene molecules can exhibit a "standing-up" or "lying-down" orientation depending on the nature of the underlying surface, 5-7 TIPS-PEN molecules invariably adopt a molecular orientation in which the silyl groups contact the substrate surface.⁸⁻¹⁸ Consequently, the high-mobility π -stack direction lies parallel to the substrate surface, an orientation that has been widely observed across this class of compounds, including those derivatized with alkyl side chains. 19,20

While aligning the high-mobility π -stack direction with the underlying substrate surface is ideal for charge transport between coplanar source and drain electrodes in OFETs, other optoelectronic devices, such as organic solar cells, organic

Received: March 12, 2019 Revised: April 16, 2019 Published: April 29, 2019

3461

Department of Chemical Engineering and Materials Science, Stevens Institute of Technology, Hoboken, New Jersey 07030, United

[‡]Department of Physics, Stevens Institute of Technology, Hoboken, New Jersey 07030, United States

[§]Department of Polymer Science and Engineering, University of Massachusetts Amherst, Amherst, Massachusetts 01003, United

Department of Chemistry, New York University, New York, New York 10002, United States

Figure 1. (A, B) Side-view SEM images of a TIPS-PY film dip-coated onto a SiO_2 substrate and an AAO scaffold, respectively. The dashed red lines in (B) indicate the AAO scaffold. Insets display side-view SEM images at a tilt angle of 35° of a flat SiO_2/Si substrate and a nanoporous AAO scaffold formed on SiO_2 in which the pores partially connect, respectively.

light-emitting diodes, and vertical field-effect transistors, require charge transport to occur perpendicular to the substrate surface. For these devices, the orientation adopted by TIPS-PEN and other soluble small-molecule organic semiconductors results in poor out-of-plane charge transport, as charges must hop across the insulating side groups that render the molecules soluble. Using a novel derivative with a large aromatic core of nine fused benzene rings, TIPSpyranthrene (TIPS-PY), we recently demonstrated the ability to control the out-of-plane orientation of these molecules by tuning the surface energy of the underlying substrate.² Specifically, low surface energy substrates promoted aromatic core-substrate interactions, such that the molecules rotated ~90°. Conductive atomic force microscopy experiments revealed this change in orientation to correspond to a 2order of magnitude improvement in the out-of-plane hole mobility of TIPS-PY crystals, from 10⁻⁷ to 10⁻⁵ cm²/V·s.

Still, both of the molecular orientations of TIPS-PY crystals in the above work resulted in the π -stack direction lying parallel to the substrate surface. The ideal molecular orientation for devices using sandwich electrode structures is one in which the π -stack direction lies perpendicular to the substrate surface. Solar cells comprising thermally evaporated pentacene with a "lying-down" orientation (i.e., the π -stack direction perpendicular to the substrate surface) exhibited power conversion efficiencies of almost 4%, compared to less than 1% for solar cells comprising pentacene molecules in a "standing-up" orientation (i.e., the π -stack direction parallel to the substrate surface). 5-7,22 Similar observations have been reported for thermally evaporated zinc- and copper-phthalocyanine-based devices. 23-27 In solution-processed smallmolecule systems, however, the lying-down orientation has rarely been reported. In 2015, Kaner and co-workers demonstrated the solution-phase growth of phenyl/phenylcapped tetraaniline vertical crystals with the π -stack direction perpendicular to the substrate surface using graphene to direct molecular orientation.²⁸ Successful use of graphene to control out-of-plane molecular orientation in functionalized smallmolecule organic semiconductors, however, has not yet been reported, with $\pi - \pi$ interactions between the molecules and underlying substrate hindered by prohibitively large solubilizing side groups.

To address this critical issue of out-of-plane orientation control in solution-processable small-molecule organic semi-conductors, we herein present a novel, generalizable strategy to fabricate arrays of vertical single crystals in which the π -stack direction is perpendicular to the substrate surface. Specifically, we use nanostructured anodized aluminum oxide (AAO)

scaffolds to guide the earliest stages of crystallization at the solvent-substrate-air interface as solvent evaporates during film deposition. This strategy centers on the general principle that crystals formed within two-dimensionally nanoconfined spaces tend to grow with their fast growth direction along the third, unconfined axis (e.g., the long axis of cylindrical pores). In organic semiconductors, the fast growth direction typically corresponds to the π -stack direction. Using nanoporous AAO scaffolds exhibiting uniaxially aligned pores perpendicular to the substrate surface, we select for nuclei oriented with the π stack direction also perpendicular to the substrate surface. Significantly, our method does not require the removal of the directing scaffold to expose the crystal surfaces, as crystal growth proceeds above the scaffold surface. These scaffolds can be incorporated onto both rigid and flexible supports, including paper,²⁹ polyethylene naphthalate (PEN),³⁰ and polyimide (PI),³⁰ for potential use in rollable displays and solar panels. Furthermore, our tunable dip-coating process to deposit the vertical crystal arrays is compatible with largearea, high-throughput manufacturing methods. Photoluminescence (PL) measurements have revealed a dramatically enhanced PL signal at the crystal tips exposing the high surface energy π -planes.

■ EXPERIMENTAL SECTION

Synthesis of Chemical Compounds. Bis(triisopropylsilylethynyl)pentacene (TIPS-PEN) and 5,11-bis(triethylsilylethynyl)anthradithiophene (TES-ADT) were purchased from Sigma-Aldrich company (≥99% purity). Bis(TIPS)dibenzopyrene (TIPS-DBP), bis(TIPS)anthanthrene (TIPS-AT), bis(TIPS)bistetracene (TIPS-BT), and bis(TIPS)pyranthrene (TIPS-PY) were synthesized according to previously published procedures.³¹

Preparation of Anodic Aluminum Oxide (AAO) Scaffolds. First, 200 nm of Al was thermally evaporated onto clean SiO_2/Si substrates. The film was then anodized for 150 s in an aqueous solution of 0.3 M oxalic acid ($H_2C_2O_4$) at a potential ranging from 30 to 80 V and a reaction temperature of 13 °C. During this process, cylindrical pores with average diameters of 60–200 nm were formed, depending on the applied voltage. The anodized Al films were then further etched in an aqueous 0.3 M phosphoric acid (H_3PO_4) solution maintained at 30 °C to widen the pores until they partially coalesced.

Vertical Crystal Array Formation via Continuous Dip-Coating. AAO scaffolds were immersed in organic semiconductor solutions at concentrations of 0.25 wt % in toluene and a temperature of 80 °C. A syringe pump was used to withdraw the samples at rates ranging from 0.4 to 1.0 mm/min. The solutions were covered with aluminum foil to prevent solvent evaporation during the process.

Indexing of Crystallographic Faces. A TIPS-PY solution at a concentration of 0.25 wt % in toluene was prepared in a vial, and the solvent was allowed to slowly evaporate overnight. The needle-like TIPS-PY crystals were collected by ultrasonication for 15 min in

ethanol and dried at 100 °C. A crystal was mounted on a 0.15 mm MiTeGen MicroMount loop for X-ray diffraction measurements. Indexing of the crystal faces was performed on a Bruker SMART APEX II diffractometer equipped with a CCD detector with an incident X-ray wavelength of 0.71073 Å (Mo-K α). The crystal temperature was maintained at 100 K during measurements using an Oxford Cryosystems 700+ Cooler. Three sets of matrix runs including 12 two-dimensional diffraction images per run were collected for unit cell determination.

Photoluminescence (PL) Measurements. Photoluminescence spectra were recorded with a 532 nm laser diode that was focused with a microscope objective (numerical aperture: NA = 0.55) to a near resolution-limited spot size of 1.5 μ m. The optical emission was dispersed through a spectrometer and recorded by a silicon CCD camera. For time-resolved PL measurements, we used a pulsed laser operating at 405 nm with a 20 MHz repetition rate and 100 ps pulse length. Time-correlated single-photon counting (TCSPC) experiments were carried out with a coincidence counter (SensL) and an avalanche photodiode (APD).

RESULTS AND DISCUSSION

To determine the effect of the substrate structure on organic semiconductor crystallization during solution processing, we deposited TIPS-PY films onto flat SiO₂ substrates and AAO scaffolds via dip-coating. Briefly, the substrates were immersed in a solution of 0.25 wt % TIPS-PY dissolved in toluene and withdrawn vertically from the solution using a syringe pump at a rate of 0.4 mm/min. On flat SiO₂ substrates (Figure 1A, inset), TIPS-PY formed needle-like crystals that lie flat on the surface, as displayed in the side- and top-view scanning electron microscopy (SEM) images in Figure 1A and Figure S1A, respectively. This morphology is typical of many solution-processed small-molecule semiconductors deposited by spin-coating, ^{32–35} drop-casting, ^{16,36–38} and blade-coating. ^{9,39–43}

We next deposited nanoporous AAO scaffolds onto SiO₂/Si via thermal evaporation of a 200 nm Al film, followed by anodization in an acid solution at a voltage of 40 V to form cylindrical nanopores perpendicular to the substrate surface (Figure S2). The AAO scaffolds were then immersed in a phosphoric acid solution with a 0.1 wt % concentration to widen the pores. For the purpose of our experiments, we prolonged the etching time to partially coalesce the pores, as displayed in the inset image in Figure 1B. This more open morphology of AAO compared to one exhibiting isolated nanopores facilitated wetting of the solution in the nanostructured scaffold while still providing 2D confinement of the solution during deposition.

Figure 1B and Figure S1B display side- and top-view SEM images of a TIPS-PY film dip-coated onto a nanoporous AAO scaffold. While TIPS-PY again formed needle-like crystals, these crystals surprisingly oriented with their long axes perpendicular to the substrate surface. To the best of our knowledge, this formation of "vertical" crystal arrays via solution processing is the first reported for small-molecule organic semiconductors incorporating solubilizing side groups and is in stark contrast to the "horizontal" orientation of crystals deposited on flat $\mathrm{SiO}_2/\mathrm{Si}$ substrates. Uniform arrays of vertical crystals spanned areas of at least $150 \times 150 \,\mu\mathrm{m}$ (Figure S3) and can likely be improved by controlling solution pinning during the dip-coating process. Our results indicate that the surface plays a critical role in directing nucleation and crystal growth during solution-phase deposition.

Interestingly, the average diameters and heights of these vertical crystals formed on AAO were measured to be 640 nm (± 90 nm) and 6.7 μ m (± 0.6 μ m), respectively, significantly

larger than the pore diameters and height of the underlying AAO scaffold (indicated by a dashed rectangular box in Figure 1B). This observation indicates that, upon initial nucleation at the scaffold/solution interface, crystal growth then proceeds above the scaffold. Such a morphology exposes large areas of the crystal surfaces, ideal for processes such as exciton dissociation during light energy harvesting in organic solar cells.

To definitively determine the molecular orientation of TIPS-PY with respect to the long axes of the crystals, we next performed single crystal X-ray crystallography on a TIPS-PY crystal grown slowly in a supersaturated solution. Figure 2A

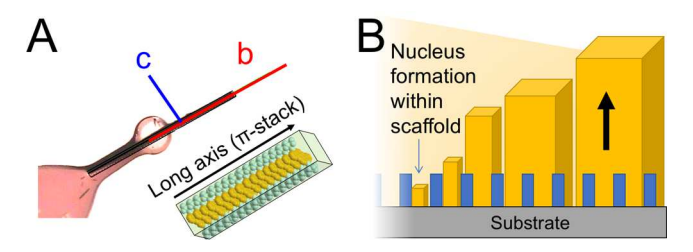


Figure 2. (A) A single TIPS-PY crystal grown from the solution-phase placed on a mounting loop for single crystal diffraction experiments, with the b and c axes relative to the crystal morphology identified. Inset displays the molecular orientation of TIPS-PY molecules with respect to the crystal morphology. (B) Scheme of TIPS-PY vertical crystal growth on nanoporous AAO scaffolds during dip-coating at the air/solution/scaffold interface.

displays the crystallographic indexing of a needle-like TIPS-PY crystal performed at 100 K, in which the b axis, or π -stack direction, was found to lie parallel to the long axis of the crystal. Collectively, our results indicate that TIPS-PY crystals nucleate within the nanopores of the AAO scaffold and proceed to grow beyond the scaffold surface, as displayed in Figure 2B. These nuclei preferentially orient with their fastest crystallographic growth direction (i.e., the π -stack direction) parallel to the long axis of the pores, and thus perpendicular to the substrate surface. Preferential orientation of crystals nanoconfined within AAO nanopores has been previously observed for a variety of molecular and polymeric systems, including glycine,44 metal-halide perovskite:solvent complexes, 45 and ferroelectric poly(vinylidene fluoride-co-trifluoroethylene). 46 In general, crystals exhibit anisotropic crystal growth rates along different crystallographic directions due to varying surface energies of crystallographic faces. To minimize their overall surface energy, crystals tend to grow fastest along the direction perpendicular to high surface energy faces. Under nanoconfinement, it is expected that only nuclei oriented with their fast growth axis parallel to the long axis of the pore can propagate beyond the critical nucleus size to form crystals.4 Unique to our system is the ability for the crystals to propagate beyond the confining scaffold to form arrays of unconfined vertical crystals with large exposed surface areas.

Aligning the π -stack direction of organic semiconductor crystals perpendicular to the substrate surface is critical for improving the performance of devices with sandwich electrode configurations because charge hopping occurs fastest along this direction. For TIPS-PEN crystals, for example, the hole mobility along the π -stack direction has been measured to be 0.14 cm²/V·s, compared to 0.045 and 0.004 cm²/V·s measured along the a and c directions, respectively. As a-and a-confining solution-phase nucleation to select for

specific crystal orientation presents an exciting generalizable strategy to optimize the out-of-plane molecular orientation of organic semiconductors. To examine the generalizability of this method to other compounds, we tested a series of six soluble acene derivatives for their growth behavior on nanoporous AAO scaffolds. Figure 3 displays top-view SEM images of the

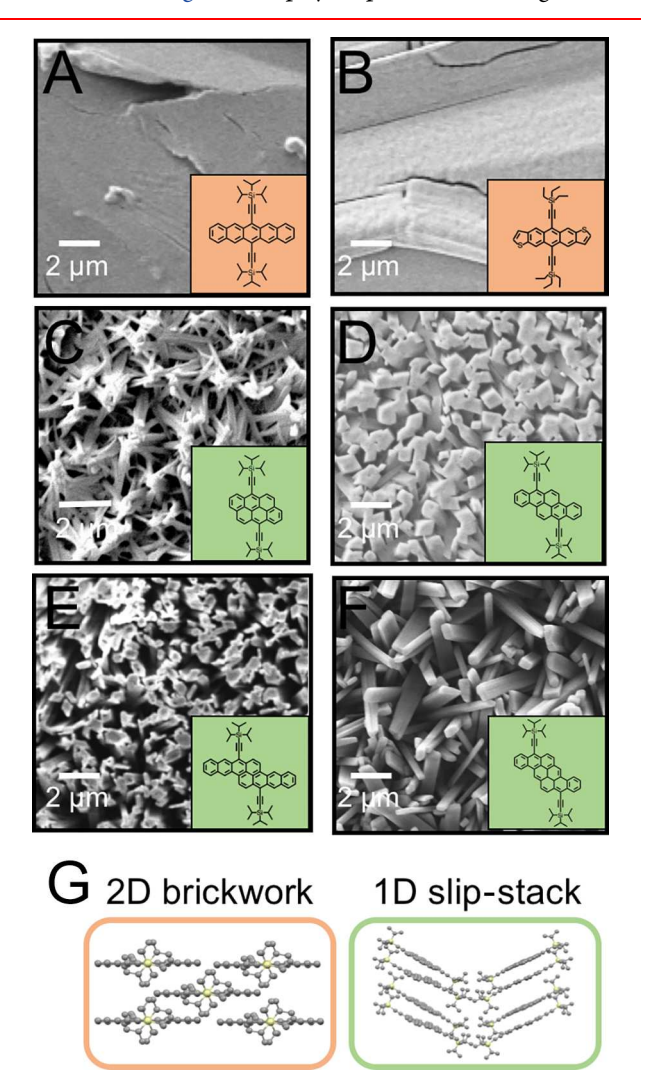


Figure 3. (A–F) Top-view SEM images of TIPS-PEN, TES-ADT, TIPS-AT, TIPS-DBP, TIPS-BT, and TIPS-PY films dip-coated onto AAO scaffolds. Molecular structures of the compounds are provided as insets. (G) 2D brickwork packing motif of TIPS-PEN and 1D slip-stack packing motif of TIPS-PY, respectively.

compounds dip-coated from solution onto AAO scaffolds, with their chemical structures displayed as insets. TIPS-PEN and bis(triethylsilylethynyl)anthradithiophene (TES-ADT), displayed in Figure 3A,B, respectively, both formed horizontal crystals on top of the AAO scaffolds. On the other hand, TIPS-anthanthrene (TIPS-AT), TIPS-dibenzopyrene (TIPS-DBP), TIPS-bistetracene (TIPS-BT), and TIPS-PY all formed arrays of vertical crystals propagating from the AAO scaffold surface (Figure 3C-F).

We speculate that the molecular packing motif adopted by the crystals is a determining factor in the direction of crystal growth, either horizontal or vertical, on nanostructured scaffolds. For such silyl-derivatized acene compounds, Anthony and co-workers have proposed a general design rule for predicting the crystal packing motif based on the size of the silyl substituent, a, and the length of the acene core, b.50 For molecules in which the a/b ratio is either less than or greater than 0.5, molecules favor a 1D slip-stack packing motif. On the other hand, for an a/b ratio of 0.5, molecules instead adopt a 2D brickwork packing motif. Figure S4 displays a schematic of a silyl-derivatived acene molecule with the a and b dimensions labeled. Of the six compounds tested, two possess an a/b ratio of approximately 0.5, namely, TES-ADT and TIPS-PEN.⁵¹ In line with the proposed molecular design rule, these compounds adopt a 2D brickwork packing motif, as displayed in Figure 3G. In this packing motif, molecules are staggered so that a π orbital of one molecule overlaps that of four other molecules. In contrast, the molecules displayed in panels C-F in Figure 3, which exhibit a/b ratios either less than or greater than 0.5, all display a 1D slip-stack packing motif in which the π -orbital of one molecule overlaps that of two other molecules (Figure S5). This packing motif strongly favors the formation of needle-like crystals and can be intentionally introduced to a system by tuning the ratio of the size of the solubilizing substituent to the acene core.50 It is also possible that other factors, such as solubility and specific molecule-substrate interactions, play a role in the mode of crystal growth, but we believe these to be secondary. We have found that dichloro-diphenyltrichloroethane, for example, forms horizontal needle-like crystals on flat surfaces but also exhibits vertical crystal growth when dipcoated onto nanoporous scaffolds (Figure S6).

While the mobilities of crystals exhibiting the 1D slip-stack motif have generally been measured to be 2–3 orders of magnitude lower than those of crystals exhibiting the 2D brickwork packing motif, we recently measured the mobility of TIPS-DBP single crystals to be 0.1 cm²/V·s along the π -stack direction.³¹ Our generalizable strategy thus is promising for the fabrication of high-performance devices with fast charge transport perpendicular to the substrate surface.

Our top-down approach of using scaffolds to direct the solution-phase nucleation of organic semiconductor crystals during film deposition provides an opportunity to further tune film parameters by adjusting the deposition conditions and scaffold structure. Using AAO nanoporous scaffolds with average pore diameters of 100 nm, we first examined the effect of the dip-coating speed on vertical TIPS-PY crystal heights and diameters. Figure 4A displays top- and side-view SEM images of a TIPS-PY film dip-coated on a nanoporous AAO scaffold at a rate of 0.4 mm/min, respectively. These crystals exhibited average diameters and heights of 640 ± 90 nm and $6.7 \pm 0.6 \mu m$, respectively. For comparison, Figure 4B displays top- and side-view SEM images of a TIPS-PY film dip-coated on a nanoporous AAO scaffold at a rate of 1.0 mm/min, respectively. As observed in the images, a faster dip-coating speed resulted in smaller crystal diameters and heights of 115 \pm 13 nm and 0.8 \pm 0.1 μ m, respectively. Figure 4C displays the average diameters and heights of TIPS-PY vertical crystals as a function of the dip-coating speed when varied from 0.4 to 1.0 mm/min. The trend of decreasing crystal dimensions with increasing dip-coating speed indicates that the dip-coating process was carried out in the evaporation regime in which molecules are deposited near the meniscus.⁵²

We also examined the effect of the characteristic pore diameter of the AAO scaffolds on vertical crystal dimensions. By varying the anodization voltage, pore sizes were varied from 60 to 200 nm (Figure S7). Figure 4D displays a graph of the average heights and diameters of TIPS-PY vertical crystals

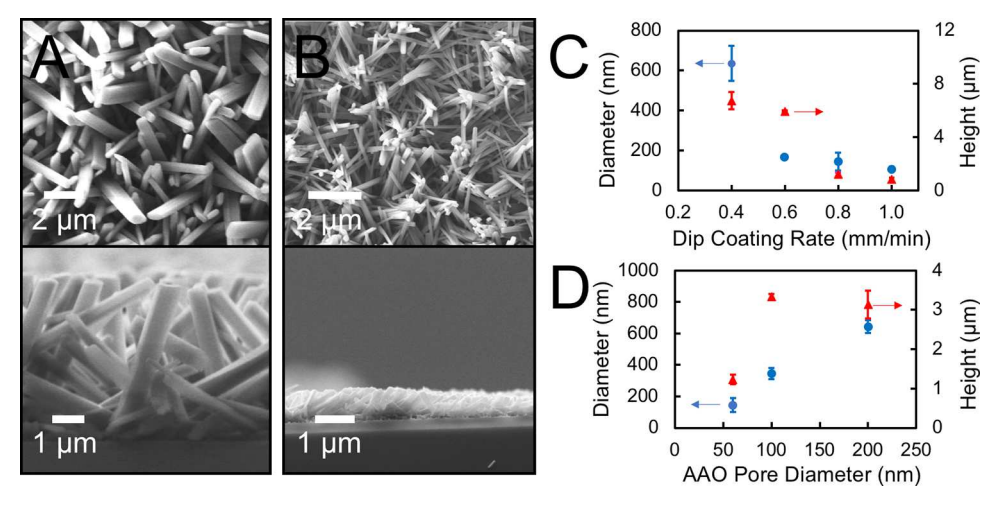


Figure 4. (A, B) Top- and side-view SEM images of TIPS-PY vertical crystals dip-coated from a 0.25 wt % solution in toluene on nanoporous AAO scaffolds with characteristic pore diameters of 100 nm at speeds of 0.4 and 1.0 mm/min, respectively. (C, D) Average diameters and lengths of TIPS-PY vertical crystals as a function of dip-coating speed and AAO pore diameters, respectively.

versus the characteristic AAO scaffold pore diameter at a fixed dip-coating rate of 1.2 mm/min (refer to Figure S8 for topand side-view SEM images). As observed from the graph, the diameters of the crystals were found to be linearly correlated to the AAO scaffold pore diameter, with smaller pore diameters resulting in smaller crystal diameters. Interestingly, the heights of TIPS-PY vertical crystals were found to be approximately the same for crystals deposited on AAO scaffolds with characteristic pore diameters of 100 and 200 nm. This observation indicates that the crystal height is primarily a function of the dip-coating speed, which in turn determines the amount of time crystals are allowed to grow at the solution-airscaffold interface before solvent evaporation-induced vitrification. It is also important to note that, for crystals grown on AAO scaffolds with a characteristic pore diameter of 200 nm, the TIPS-PY crystals tended to tilt toward the substrate surface, indicating that smaller pore diameters may be necessary to ensure the formation of vertical crystal arrays.

Interestingly, for a dip-coating speed of 1.2 mm/min, the diameters of TIPS-PY crystals were approximately 4 times larger than the confining pores in the AAO scaffold. These results indicate that not every pore acts as a nucleation site during dip-coating and that TIPS-PY crystals grow outwards above the scaffold both vertically and laterally. We hypothesize that the scaffold pore size dictates the relative nucleation density, which in turn determines the average TIPS-PY crystal diameter. The density of pores in the AAO scaffolds decreases from ~ 150 to ~ 25 pores/ μ m² as the average pore diameter increases from 60 to 200 nm, as displayed in Figure S7. Higher pore densities, which correspond to higher nucleation densities, result in decreased crystal diameters. Decreasing crystal size with increasing nucleation density is a common observation in organic semiconductor thin films, for example, in spin-coated TES-ADT films, 53,54 and across materials systems due to impingement of adjacent crystals that prevent further crystal growth.

Exposing the high surface energy π -planes at the crystal tips has important implications in the field of organic electronics. In the presence of a second semiconductor with offset energy levels, for example, exciton dissociation is expected to be most efficient at this interface. S5-61 As a demonstration of enhanced optoelectronic properties via crystal orientation control in

solution-processed organic semiconductor thin films, we measured the photoluminescence (PL) of TIPS-PY horizontally- and vertically-oriented crystals. Figure 5A displays the

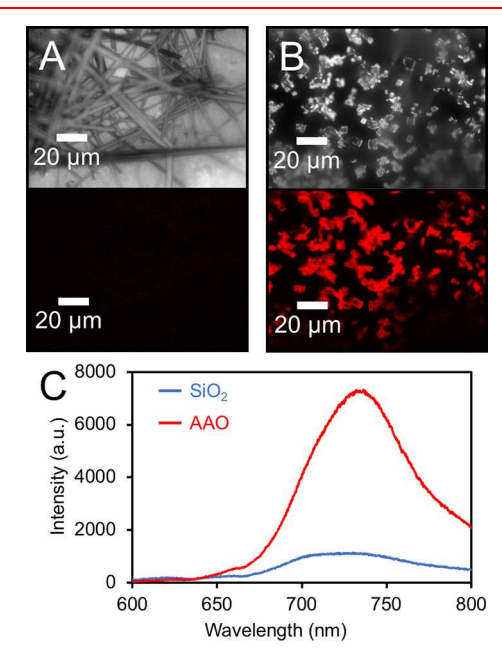


Figure 5. (A, B) Bright-field optical micrographs and corresponding fluorescence images of TIPS-PY horizontal and vertical crystals, respectively. (C) PL intensity as a function of emission wavelength collected on solid-state TIPS-PY films deposited on flat ${\rm SiO_2}$ to achieve horizontal crystals and nanoporous AAO to achieve vertical crystals at an excitation wavelength of 532 nm.

bright-field image and corresponding fluorescence image in which TIPS-PY horizontal crystals were excited with a laser operating at 532 nm. As observed in the image, the fluorescence signal from horizontal crystals is very weak.

In comparison, Figure 5B displays the bright-field and corresponding fluorescence images of TIPS-PY vertical crystals deposited on a nanoporous AAO scaffold. As observed in the fluorescence image, the PL signal is dramatically enhanced at the crystal tips that stick out of plane. To directly quantify the light enhancement at the crystal tips, we measured the PL

emission spectrum using a 532 nm laser focused down to a spot size of about 1 μ m for both horizontal and vertical crystals, as displayed in Figure 5C. By comparing peak intensities, one can estimate that the PL signal from TIPS-PY crystals in a vertical orientation is 8-fold enhanced compared to that from TIPS-PY crystals adopting a horizontal orientation on flat SiO2. One could argue that the reason for the low intensity in the horizontal configuration is that the underlying SiO₂ substrate causes nonradiative PL quenching, as found, for example, for 1D carbon nanotubes that are oriented horizontally. 62 In such a case, when nonradiative recombination is dominant, the spontaneous emission lifetime (T_1) should be drastically reduced. In contrast, we find that the T_1 times of the PL emission for both crystal configurations are unchanged, with $T_1 = 6.2$ ns, excluding detrimental substrate effects (Figure S9). We therefore attribute the 8-fold PL enhancement for TIPS-PY vertical crystals to be primarily caused by efficient waveguiding along the crystal length. Such PL intensity dependence on crystal orientation has important implications in the fields of organic light-emitting diodes, organic solar cells, and sensors.

CONCLUSIONS

Solution processing of organic semiconductors for optoelectronic devices promises to enable the high-throughput, lowcost manufacturing of flexible devices, including solar panels, displays, and sensors. However, such rapid processing is accompanied by a loss of control over the active layer morphology, which in turn largely determines overall device performance. Also inherent to solution-processable smallmolecule organic semiconductors is the inability to dictate the out-of-plane molecular orientation due to strong interactions between the solubilizing side groups and the underlying substrate. Exploiting the preference of nanoconfined crystals to orient with their fast growth direction parallel to the unconfined dimension, we have demonstrated the use of nanoporous AAO scaffolds to direct the nucleation of small-molecule organic semiconductor crystals during solution deposition. This strategy to direct nucleation within scaffolds while allowing crystal growth to propagate above the scaffolds resulted in the formation of arrays of unconfined vertical crystals with high surface area and molecular orientations optimized for light harvesting, exciton dissociation, and charge transport in sandwich-electrode device configurations. Critically, our deposition strategy is compatible with continuous processing methods that will drive down manufacturing costs and be applied to other soluble molecular compounds used in a myriad of industries, from pharmaceutics to food manufacturing.

ASSOCIATED CONTENT

S Supporting Information

The Supporting Information is available free of charge on the ACS Publications website at DOI: 10.1021/acs.cgd.9b00321.

Experimental details and additional characterization (PDF)

AUTHOR INFORMATION

Corresponding Author

*E-mail: stephanie.lee@stevens.edu.

ORCID ®

Chunhua Hu: 0000-0002-8172-2202

Stefan Strauf: 0000-0002-9887-7059 Stephanie S. Lee: 0000-0003-0964-6353

Author Contributions

The manuscript was written through contributions of all authors.

Notes

The authors declare no competing financial interest.

ACKNOWLEDGMENTS

S.S.L. acknowledges financial support from the National Science Foundation Advanced Manufacturing Program (AM-1846178). The authors also acknowledge support from the PSEG Foundation to advance energy innovation at Stevens. A.B. acknowledges the National Science Foundation (DMR-1508627). C.H. acknowledges the support of the National Science Foundation Chemistry Research Instrumentation and Facilities Program (CHE-0840277) and the Materials Research Science and Engineering Center (MRSEC) Program (DMR-1420073). Research was carried out at the Micro Device Laboratory and used SEM and confocal microscopes within the Laboratory for Multiscale Imaging at Stevens Institute of Technology. The authors also thank Dr. Tsengming Chou for assistance and Dr. Takuji Adachi and Prof. Bart Kahr for helpful discussions.

REFERENCES

- (1) Anthony, J. E.; Eaton, D. L.; Parkin, S. R. A Road Map to Stable, Soluble, Easily Crystallized Pentacene Derivatives. *Org. Lett.* **2002**, *4*, 15–18.
- (2) Anthony, J. E.; Brooks, J. S.; Eaton, D. L.; Parkin, S. R. Functionalized Pentacene: Improved Electronic Properties from Control of Solid-State Order. *J. Am. Chem. Soc.* **2001**, *123*, 9482–9483.
- (3) Yi, H. T.; Payne, M. M.; Anthony, J. E.; Podzorov, V. Ultra-Flexible Solution-Processed Organic Field-Effect Transistors. *Nat. Commun.* **2012**, *3*, 1259.
- (4) Mishra, A.; Bäuerle, P. Small Molecule Organic Semiconductors on the Move: Promises for Future Solar Energy Technology. *Angew. Chem., Int. Ed.* **2012**, *51*, 2020–2067.
- (5) Jo, S. B.; Kim, H. H.; Lee, H.; Kang, B.; Lee, S.; Sim, M.; Kim, M.; Lee, W. H.; Cho, K. Boosting Photon Harvesting in Organic Solar Cells with Highly Oriented Molecular Crystals via Graphene—Organic Heterointerface. *ACS Nano* **2015**, *9*, 8206–8219.
- (6) Kim, K.; Santos, E. J. G.; Lee, T. H.; Nishi, Y.; Bao, Z. Epitaxially Grown Strained Pentacene Thin Film on Graphene Membrane. *Small* **2015**, *11*, 2037–2043.
- (7) Mativetsky, J. M.; Wang, H.; Lee, S. S.; Whittaker-Brooks, L.; Loo, Y.-L. Face-on Stacking and Enhanced out-of-Plane Hole Mobility in Graphene-Templated Copper Phthalocyanine. *Chem. Commun.* **2014**, *50*, 5319–5321.
- (8) Chen, J.; Tee, C. K.; Shtein, M.; Martin, D. C.; Anthony, J. Controlled Solution Deposition and Systematic Study of Charge-Transport Anisotropy in Single Crystal and Single-Crystal Textured TIPS Pentacene Thin Films. *Org. Electron.* **2009**, *10*, 696–703.
- (9) Giri, G.; Verploegen, E.; Mannsfeld, S. C. B.; Atahan-Evrenk, S.; Kim, D. H.; Lee, S. Y.; Becerril, H. A.; Aspuru-Guzik, A.; Toney, M. F.; Bao, Z. Tuning Charge Transport in Solution-Sheared Organic Semiconductors Using Lattice Strain. *Nature* **2011**, *480*, 504–508.
- (10) Zheng, F.; Park, B. N.; Seo, S.; Evans, P. G.; Himpsel, F. J. Orientation of Pentacene Molecules on SiO2: From a Monolayer to the Bulk. *J. Chem. Phys.* **2007**, *126*, 154702.
- (11) Sakamoto, K.; Ueno, J.; Bulgarevich, K.; Miki, K. Anisotropic Charge Transport and Contact Resistance of 6,13- Bis-(Triisopropylsilylethynyl) Pentacene Field-Effect Transistors Fabricated by a Modified Flow-Coating Method. *Appl. Phys. Lett.* **2012**, 100, 123301.

(12) He, Z.; Xiao, K.; Durant, W.; Hensley, D. K.; Anthony, J. E.; Hong, K.; Kilbey, S. M.; Chen, J.; Li, D. Enhanced Performance Consistency in Nanoparticle/TIPS Pentacene-Based Organic Thin Film Transistors. *Adv. Funct. Mater.* **2011**, *21*, 3617–3623.

- (13) Chen, J.; Martin, D. C.; Anthony, J. E. Morphology and Molecular Orientation of Thin-Film Bis(Triisopropylsilylethynyl) Pentacene. *J. Mater. Res.* **2007**, *22*, 1701–1709.
- (14) Fritz, S. E.; Martin, S. M.; Frisbie, C. D.; Ward, M. D.; Toney, M. F. Structural Characterization of a Pentacene Monolayer on an Amorphous SiO2 Substrate with Grazing Incidence X-Ray Diffraction. *J. Am. Chem. Soc.* **2004**, *126*, 4084–4085.
- (15) Li, Y.; Sun, H.; Shi, Y.; Tsukagoshi, K. Patterning Technology for Solution-Processed Organic Crystal Field-Effect Transistors. *Sci. Technol. Adv. Mater.* **2014**, *15*, 024203.
- (16) Mukherjee, B. Organic Phototransistor from Solution Cast, Ordered Crystals Assembly of a Pentacene Derivative. *Indian J. Phys.* **2014**, *88*, 1073–1079.
- (17) Rogowski, R. Z.; Dzwilewski, A.; Kemerink, M.; Darhuber, A. A. Solution Processing of Semiconducting Organic Molecules for Tailored Charge Transport Properties. *J. Phys. Chem. C* **2011**, *115*, 11758–11762.
- (18) Chen, W.; Huang, H.; Thye, A.; Wee, S.; Weiss, H.; Rabe, J. P.; Wee, A. T. S.; Zhang, K. P.; Chen, Z. K.; Wee, A. T. S.; Renner, C.; Aeppli, G. Molecular Orientation Transition of Organic Thin Films on Graphite: The Effect of Intermolecular Electrostatic and Interfacial Dispersion Forces. *Chem. Commun.* **2008**, 93, 4276.
- (19) Naito, R.; Toyoshima, S.; Ohashi, T.; Sakurai, T.; Akimoto, K. Molecular Orientation Control of Phthalocyanine Thin Film by Inserting Pentacene Buffer Layer. *Jpn. J. Appl. Phys.* **2008**, 47, 1416–1418.
- (20) McGarry, K. A.; Xie, W.; Sutton, C.; Risko, C.; Wu, Y.; Young, V. G.; Brédas, J. L.; Frisbie, C. D.; Douglas, C. J. Rubrene-Based Single-Crystal Organic Semiconductors: Synthesis, Electronic Structure, and Charge-Transport Properties. *Chem. Mater.* **2013**, 25, 2254–2263.
- (21) Bai, X.; Zong, K.; Ly, J.; Mehta, J. S.; Hand, M.; Molnar, K.; Lee, S. S.; Kahr, B.; Mativetsky, J. M.; Briseno, A.; Lee, S. S. Orientation Control of Solution-Processed Organic Semiconductor Crystals To Improve Out-of-Plane Charge Mobility. *Chem. Mater.* **2017**, 29, 7571–7578.
- (22) Zhang, Y.; Diao, Y.; Lee, H.; Mirabito, T. J.; Johnson, R. W.; Puodziukynaite, E.; John, J.; Carter, K. R.; Emrick, T.; Mannsfeld, S. C. B.; Briseno, A. L. Intrinsic and Extrinsic Parameters for Controlling the Growth of Organic Single-Crystalline Nanopillars in Photovoltaics. *Nano Lett.* **2014**, *14*, 5547–5554.
- (23) Chu, C.-W.; Shrotriya, V.; Li, G.; Yang, Y. Tuning Acceptor Energy Level for Efficient Charge Collection in Copper-Phthalocyanine-Based Organic Solar Cells. *Appl. Phys. Lett.* **2006**, *88*, 153504.
- (24) Feng, C.; Yi, M.; Yu, S.; Ma, D.; Feng, C.; Zhang, T.; Meruvia, M. S.; Hümmelgen, I. A. Copper Phthalocyanine Based Hybrid P-Type Permeable-Base Transistor in Vertical Architecture. *Appl. Phys. Lett.* **2006**, *88*, 203501.
- (25) Singh, V. P.; Singh, R. S.; Parthasarathy, B.; Aguilera, A.; Anthony, J.; Payne, M. Copper-Phthalocyanine-Based Organic Solar Cells with High Open-Circuit Voltage. *Appl. Phys. Lett.* **2005**, *86*, 082106.
- (26) Gonzalez Arellano, D. L.; Burnett, E. K.; Demirci Uzun, S.; Zakashansky, J. A.; Champagne, V. K.; George, M.; Mannsfeld, S. C. B.; Briseno, A. L. Phase Transition of Graphene-Templated Vertical Zinc Phthalocyanine Nanopillars. *J. Am. Chem. Soc.* **2018**, *140*, 8185–8191
- (27) Gonzalez Arellano, D. L.; Kolewe, K. W.; Champagne, V. K.; Kurtz, I. S.; Burnett, E. K.; Zakashansky, J. A.; Arisoy, F. D.; Briseno, A. L.; Schiffman, J. D. Gecko-Inspired Biocidal Organic Nanocrystals Initiated from a Pencil-Drawn Graphite Template. *Sci. Rep.* **2018**, *8*, 11618.
- (28) Wang, Y.; Torres, J. A.; Stieg, A. Z.; Jiang, S.; Yeung, M. T.; Rubin, Y.; Chaudhuri, S.; Duan, X.; Kaner, R. B. Graphene-Assisted

Solution Growth of Vertically Oriented Organic Semiconducting Single Crystals. ACS Nano 2015, 9, 9486–9496.

- (29) Balde, M.; Vena, A.; Sorli, B. Fabrication of Porous Anodic Aluminium Oxide Layers on Paper for Humidity Sensors. *Sens. Actuators, B* **2015**, 220, 829–839.
- (30) Kaltenbrunner, M.; Stadler, P.; Schwödiauer, R.; Hassel, A. W.; Sariciftci, N. S.; Bauer, S. Anodized Aluminum Oxide Thin Films for Room-Temperature-Processed, Flexible, Low-Voltage Organic Non-Volatile Memory Elements with Excellent Charge Retention. *Adv. Mater.* **2011**, 23, 4892–4896.
- (31) Zhang, L.; Fonari, A.; Zhang, Y.; Zhao, G.; Coropceanu, V.; Hu, W.; Parkin, S.; Brédas, J.-L.; Briseno, A. L. Triisopropylsilylethynyl-Functionalized Graphene-Like Fragment Semiconductors: Synthesis, Crystal Packing, and Density Functional Theory Calculations. *Chem. Eur. J.* **2013**, *19*, 17907–17916.
- (32) Akkerman, H. B.; Chang, A. C.; Verploegen, E.; Bettinger, C. J.; Toney, M. F.; Bao, Z. Fabrication of Organic Semiconductor Crystalline Thin Films and Crystals from Solution by Confined Crystallization. *Org. Electron.* **2012**, *13*, 235–243.
- (33) Poornachary, S. K.; Parambil, J. V.; Chow, P. S.; Tan, R. B. H.; Heng, J. Y. Y. Nucleation of Elusive Crystal Polymorphs at the Solution—Substrate Contact Line. *Cryst. Growth Des.* **2013**, *13*, 1180—1186
- (34) Liu, C.; Minari, T.; Li, Y.; Kumatani, A.; Lee, M. V.; Athena Pan, S. H.; Takimiya, K.; Tsukagoshi, K. Direct Formation of Organic Semiconducting Single Crystals by Solvent Vapor Annealing on a Polymer Base Film. *J. Mater. Chem.* **2012**, 22, 8462.
- (35) Li, Y.; Liu, C.; Lee, M. V.; Xu, Y.; Wang, X.; Shi, Y.; Tsukagoshi, K. In Situpurification to Eliminate the Influence of Impurities in Solution-Processed Organic Crystals for Transistor Arrays. J. Mater. Chem. C 2013, 1, 1352–1358.
- (36) Lee, J. H.; Seo, Y.; Park, Y. D.; Anthony, J. E.; Kwak, D. H.; Lim, J. A.; Ko, S.; Jang, H. W.; Cho, K.; Lee, W. H. Effect of Crystallization Modes in TIPS-Pentacene/Insulating Polymer Blends on the Gas Sensing Properties of Organic Field-Effect Transistors. *Sci. Rep.* **2019**, *9*, 21.
- (37) Tan, L.; Jiang, W.; Jiang, L.; Jiang, S.; Wang, Z.; Yan, S.; Hu, W. Single Crystalline Microribbons of Perylo[1,12-b,c,d]Selenophene for High Performance Transistors. *Appl. Phys. Lett.* **2009**, *94*, 153306.
- (38) Li, H.; Tee, B. C.-K.; Cha, J. J.; Cui, Y.; Chung, J. W.; Lee, S. Y.; Bao, Z. High-Mobility Field-Effect Transistors from Large-Area Solution-Grown Aligned C ₆₀ Single Crystals. *J. Am. Chem. Soc.* **2012**, 134, 2760–2765.
- (39) Niazi, M. R.; Li, R.; Qiang Li, E.; Kirmani, A. R.; Abdelsamie, M.; Wang, Q.; Pan, W.; Payne, M. M.; Anthony, J. E.; Smilgies, D.-M.; Thoroddsen, S. T.; Giannelis, E. P.; Amassian, A. Solution-Printed Organic Semiconductor Blends Exhibiting Transport Properties on Par with Single Crystals. *Nat. Commun.* **2015**, *6*, 8598.
- (40) Giri, G.; Park, S.; Vosgueritchian, M.; Shulaker, M. M.; Bao, Z. High-Mobility, Aligned Crystalline Domains of TIPS-Pentacene with Metastable Polymorphs Through Lateral Confinement of Crystal Growth. *Adv. Mater.* **2014**, *26*, 487–493.
- (41) Diao, Y.; Tee, B. C.-K.; Giri, G.; Xu, J.; Kim, D. H.; Becerril, H. a; Stoltenberg, R. M.; Lee, T. H.; Xue, G.; Mannsfeld, S. C. B.; Bao, Z. Solution Coating of Large-Area Organic Semiconductor Thin Films with Aligned Single-Crystalline Domains. *Nat. Mater.* **2013**, *12*, 665–671
- (42) Pisula, W.; Menon, A.; Stepputat, M.; Lieberwirth, I.; Kolb, U.; Tracz, A.; Sirringhaus, H.; Pakula, T.; Müllen, K. A Zone-Casting Technique for Device Fabrication of Field-Effect Transistors Based on Discotic Hexa- *Peri* -Hexabenzocoronene. *Adv. Mater.* **2005**, *17*, 684–689
- (43) Wo, S.; Headrick, R. L.; Anthony, J. E. Fabrication and Characterization of Controllable Grain Boundary Arrays in Solution-Processed Small Molecule Organic Semiconductor Films. *J. Appl. Phys.* **2012**, *111*, 073716.
- (44) Hamilton, B. D.; Weissbuch, I.; Lahav, M.; Hillmyer, M. a; Ward, M. D. Manipulating Crystal Orientation in Nanoscale

Cylindrical Pores by Stereochemical Inhibition. J. Am. Chem. Soc. 2009, 131, 2588–2596.

- (45) Lee, S.; Feldman, J.; Lee, S. S. Nanoconfined Crystallization of MAPbI 3 to Probe Crystal Evolution and Stability. *Cryst. Growth Des.* **2016**, *16*, 4744–4751.
- (46) García-Gutiérrez, M.-C.; Linares, A.; Hernández, J. J.; Rueda, D. R.; Ezquerra, T. A.; Poza, P.; Davies, R. J. Confinement-Induced One-Dimensional Ferroelectric Polymer Arrays. *Nano Lett.* **2010**, *10*, 1472–1476.
- (47) Jiang, Q.; Ward, M. D. Crystallization under Nanoscale Confinement. *Chem. Soc. Rev.* **2014**, *43*, 2066–2079.
- (48) Sundar, V. C.; Zaumseil, J.; Podzorov, V.; Menard, E.; Willett, R. L.; Someya, T.; Gershenson, M. E.; Rogers, J. a. Elastomeric Transistor Stamps: Reversible Probing of Charge Transport in Organic Crystals. *Science (Washington, DC, U. S.)* **2004**, 303, 1644–1646
- (49) Headrick, R. L.; Wo, S.; Sansoz, F.; Anthony, J. E. Anisotropic Mobility in Large Grain Size Solution Processed Organic Semiconductor Thin Films. *Appl. Phys. Lett.* **2008**, *92*, 063302.
- (50) Anthony, J. E. Functionalized Acenes and Heteroacenes for Organic Electronics. *Chem. Rev.* **2006**, *106*, 5028–5048.
- (\$1) Subramanian, S.; Park, S. K.; Parkin, S. R.; Podzorov, V.; Jackson, T. N.; Anthony, J. E. Chromophore Fluorination Enhances Crystallization and Stability of Soluble Anthradithiophene Semiconductors. *J. Am. Chem. Soc.* **2008**, *130*, 2706–2707.
- (52) Le Berre, M.; Chen, Y.; Baigl, D. From Convective Assembly to Landau–Levich Deposition of Multilayered Phospholipid Films of Controlled Thickness. *Langmuir* **2009**, *25*, 2554–2557.
- (53) Lee, S. S.; Muralidharan, S.; Woll, A. R.; Loth, M. A.; Li, Z.; Anthony, J. E.; Haataja, M.; Loo, Y. L. Understanding Heterogeneous Nucleation in Binary, Solution-Processed, Organic Semiconductor Thin Films. *Chem. Mater.* **2012**, *24*, 2920–2928.
- (54) Lee, S. S.; Kim, C. S.; Gomez, E. D.; Purushothaman, B.; Toney, M. F.; Wang, C.; Hexemer, A.; Anthony, J. E.; Loo, Y.-L. Controlling Nucleation and Crystallization in Solution-Processed Organic Semiconductors for Thin-Film Transistors. *Adv. Mater.* **2009**, 21, 3605–3609.
- (55) Rand, B. P.; Burk, D. P.; Forrest, S. R. Offset Energies at Organic Semiconductor Heterojunctions and Their Influence on the Open-Circuit Voltage of Thin-Film Solar Cells. *Phys. Rev. B: Condens. Matter Mater. Phys.* **2007**, *75*, 115327.
- (56) Baranovskii, S. D.; Wiemer, M.; Nenashev, A. V.; Jansson, F.; Gebhard, F. Calculating the Efficiency of Exciton Dissociation at the Interface between a Conjugated Polymer and an Electron Acceptor. *J. Phys. Chem. Lett.* **2012**, *3*, 1214–1221.
- (57) Wiemer, M.; Nenashev, A. V.; Jansson, F.; Baranovskii, S. D. On the Efficiency of Exciton Dissociation at the Interface between a Conjugated Polymer and an Electron Acceptor. *Appl. Phys. Lett.* **2011**, 99, 013302.
- (58) Bindl, D. J.; Safron, N. S.; Arnold, M. S. Dissociating Excitons Photogenerated in Semiconducting Carbon Nanotubes at Polymeric Photovoltaic Heterojunction Interfaces. *ACS Nano* **2010**, *4*, 5657–5664
- (59) Lloyd, M. T.; Lim, Y.-F.; Malliaras, G. G. Two-Step Exciton Dissociation in Poly(3-Hexylthiophene)/Fullerene Heterojunctions. *Appl. Phys. Lett.* **2008**, *92*, 143308.
- (60) Marchiori, C. F. N.; Koehler, M. Dipole Assisted Exciton Dissociation at Conjugated Polymer/Fullerene Photovoltaic Interfaces: A Molecular Study Using Density Functional Theory Calculations. *Synth. Met.* **2010**, *160*, 643–650.
- (61) Nenashev, A. V.; Wiemer, M.; Jansson, F.; Baranovskii, S. D. Theory to Exciton Dissociation at the Interface between a Conjugated Polymer and an Electron Acceptor. *J. Non-Cryst. Solids* **2012**, 358, 2508–2511.
- (62) Sarpkaya, I.; Zhang, Z.; Walden-Newman, W.; Wang, X.; Hone, J.; Wong, C. W.; Strauf, S. Prolonged Spontaneous Emission and Dephasing of Localized Excitons in Air-Bridged Carbon Nanotubes. *Nat. Commun.* **2013**, *4*, 2152.